

Pseudogap phase formation in the crossover from Bose-Einstein condensation to BCS superconductivity

V.P. Gusynin¹, V.M. Loktev¹ and S.G. Sharapov^{1,2}

¹*Bogolyubov Institute for Theoretical Physics,
252143 Kiev, Ukraine*

²*Department of Physics, University of Pretoria,
0002 Pretoria, South Africa*

(September 3, 1997)

Abstract

It is shown that a phase diagram of a 2D metal with variable carrier density consists of the regions of normal phase, where the order parameter is absent; so called “abnormal normal” phase where this parameter is also absent but the mean number of composite bosons (bound pairs) exceeds the mean number of free fermions; pseudogap phase where the absolute value of the order parameter has been gradually formed but its phase is a random value, and at last superconducting (here Berezinskii-Kosterlitz-Thouless) phase. The characteristic temperatures of the transitions between these phases are found. The chemical potential and paramagnetic susceptibility behavior as functions of the fermion density and the temperature is also studied. The attempt is made to compare qualitatively the phase diagram obtained with features of behavior observed in underdoped high- T_c superconducting compounds above their critical temperature.

74.72.-h, 74.20.Fg, 74.20.Mn, 64.60.Cn

I. INTRODUCTION

Studying of a crossover region between superconductivity of Cooper pairs and superfluidity of composite bosons attracts much attention due to its close relation to a more general problem of the description of high-temperature superconductors (HTSC) (see e.g. [1,2]). At present there is understanding of this region for 3D systems at zero and finite temperatures [3]. The crossover in quasi-2D systems was, though not fully, also studied [4], whereas for 2D systems only the case of $T = 0$ [3,5] was addressed. The latter, as is known, is related to the fact that fluctuations of a charged complex order parameter in 2D systems are so large, that they destroy the long range order at any finite temperature (Coleman-Mermin-Wagner-Hohenberg's theorem [6]). In this case the appearance of an inhomogeneous condensate with a power decay of the correlations (so called Berezinskii-Kosterlitz-Thouless (BKT) phase) is possible. But its adequate mathematical description involves some difficulties.

Most of previous analyses [7–9] of the behavior of the 2D systems at $T \neq 0$ have been based on a Nozières-Schmitt-Rink approach [10]. This approach is simply the Gaussian approximation to the functional integral that perhaps explains the difficulties faced in these calculations. On the one hand, Gaussian fluctuations destroy long-range order in 2D and if one searches for the T_c^{2D} at which the order sets in one should get zero in accordance with the above-mentioned theorems [6]. On the other hand, taking into account Gaussian fluctuations is completely inadequate to describe the BKT transition [11].

Nonetheless, several steps have been made even in this direction. For example, the BKT transition in the relativistic $2 + 1$ -theory was studied in [12], and even the crossover from superconductivity to superfluidity was considered in [13] (see also [14]) as a function of the carrier density n_f . However, the method employed in [13] to obtain the temperature T_{BKT} has a number of drawbacks. Specifically, the equation for T_{BKT} was obtained neglecting the existence of a neutral (real) order parameter ρ whose appearance at finite T , being connected with the breaking of a discrete symmetry, is not inconsistent with Coleman-Mermin-Wagner-Hohenberg theorem.

As we shall see below, ρ defines the modulus of a multivalued complex order parameter of a 2D systems, and only the latter determines the possibility of the formation of nonuniform (including vortex) configurations in the system. However, as a result of allowing for a neutral order parameter, a region where ρ decays gradually to zero appears in the phase diagram of the system. This region separates the standard normal phase with $\rho = 0$ from the BKT phase, where there is the power decay of correlations. Despite of the exponential decay of the correlations in it, this new region of states very likely possesses unusual properties, since ρ appears in all expressions in the same manner as does the energy gap Δ in the theory of ordinary superconductors, though to calculate the observed single-particle spectrum, of course, the carrier losses due to scattering of carriers by fluctuations of the phase of the order parameter and, in case of real systems, by dopants must be taken into account [15]. The possible existence of such a phase, which is also in some sense normal, might shed light on the frequently anomalous (see, for example, the reviews [1,16]) behavior of the normal state of HTSC, specifically, the temperature dependencies of the spin susceptibility, resistivity, specific heat, photoemission spectra, and so on [17,18], for the explanation of which the idea of a pseudogap (and also spin gap) in the region $T > T_c$ is now widely employed.

Thus, our main objective in this article is to calculate T_{BKT} and T_ρ (T_ρ is the temperature

at which $\rho \rightarrow 0$) self-consistently as functions of n_f and to establish a form of this new region, which lies in the temperature interval $T_{BKT} < T < T_\rho$.

The rest of this paper is organized as follows. In Sec. II we introduce our model and sketch the formalism applied. The equation for T_{BKT} is derived in Sec. III. (The details of the calculation are discussed in Appendix A.) The equation for T_{BKT} should be solved self-consistently with the equations for ρ and chemical potential μ . Thus these equations and the equation for T_ρ are derived in Sec. IV using the effective potential, which obtained in Appendix B. The difference between used often [3,2] the pairing temperature T_P and introduced here T_ρ is discussed in Sec. V. Using the example of the static spin susceptibility it is shown in Sec. VI that the obtained pseudogap phase may really be used to explain the above-mentioned anomalous properties of the HTSC. Some useful series is derived in Appendix C.

II. THEORETICAL FRAMEWORK

The simplest model Hamiltonian for fermions which are confined to a 2D volume v reads [3-5,7]

$$H = \psi_\sigma^\dagger(x) \left(-\frac{\nabla^2}{2m} - \mu \right) \psi_\sigma(x) - V \psi_\uparrow^\dagger(x) \psi_\downarrow^\dagger(x) \psi_\downarrow(x) \psi_\uparrow(x), \quad (1)$$

where $x \equiv \mathbf{r}, \tau$; $\psi_\sigma(x)$ is a fermion field, m is an effective mass of fermions, μ is a chemical potential, V is an effective local attraction constant; one also assumes that $\hbar = k_B = 1$.

The Hubbard-Stratonovich method, which is standard for such kind of problems (see e.g. [5]), was applied to obtain the phase diagram [19]. In this method the statistical sum $Z(v, \mu, T)$ is given as a functional integral over fermi-fields (Nambu spinors) and the auxiliary field $\Phi = V \psi_\uparrow^\dagger \psi_\downarrow^\dagger$. Contrary to the usual way of calculation of Z in Φ, Φ^* variables, the parametrization $\Phi(x) = \rho(x) \exp[-i2\theta(x)]$ would be appropriate for presenting the corresponding integral [20,21]. As this replacement to modulus-phase variables takes place, it is evident that one has also to replace $\psi_\sigma(x) = \chi_\sigma(x) \exp[i\theta(x)]$. As a result one obtains

$$Z(v, \mu, T) = \int \rho \mathcal{D}\rho \mathcal{D}\theta \exp[-\beta\Omega(v, \mu, T, \rho(x), \partial\theta(x))], \quad (2)$$

where

$$\beta\Omega(v, \mu, T, \rho(x), \partial\theta(x)) = \frac{1}{V} \int_0^\beta d\tau \int d\mathbf{r} \rho^2(x) - \text{Tr} \text{Ln}G^{-1} + \text{Tr} \text{Ln}G_0^{-1} \quad (3)$$

is the one-loop effective action, which depends on the modulus-phase variables. The action (3) is expressed through the Green function of the initial (charged) fermions that has in the new variables the following operator form

$$G^{-1} = -\hat{I}\partial_\tau + \tau_3 \left(\frac{\nabla^2}{2m} + \mu \right) + \tau_1 \rho(\tau, \mathbf{r}) - \tau_3 \left[i\partial_\tau \theta(\tau, \mathbf{r}) + \frac{(\nabla\theta(\tau, \mathbf{r}))^2}{2m} \right] + \hat{I} \left[\frac{i\nabla^2\theta(\tau, \mathbf{r})}{2m} + \frac{i\nabla\theta(\tau, \mathbf{r})\nabla}{m} \right]. \quad (4)$$

The free fermion Green function $G_0 = G|_{\mu,\rho,\theta=0}$ provides the convenient regularization in the process of calculation. It is important that neither the smallness nor slowness of the variation of the phase of the order parameter was assumed in obtaining expression (4). In other words it is formally exact.

Since the low-energy dynamics in the phases in which $\rho \neq 0$ is determined mainly by the long-wavelength fluctuations of $\theta(x)$, only the lowest order derivatives of the phase need be retained in the expansion of $\Omega(v, \mu, T, \rho(x), \partial\theta(x))$:

$$\Omega(v, \mu, \rho(x), \partial\theta(x)) \simeq \Omega_{kin}(v, \mu, T, \rho, \partial\theta(x)) + \Omega_{pot}(v, \mu, T, \rho) \quad (5)$$

where

$$\Omega_{kin}(v, \mu, T, \rho, \partial\theta(x)) = T\text{Tr} \sum_{n=1}^{\infty} \frac{1}{n} (\mathcal{G}\Sigma)^n \Big|_{\rho=const} \quad (6)$$

and

$$\Omega_{pot}(v, \mu, T, \rho) = \left(\frac{1}{V} \int d\mathbf{r} \rho^2 - T\text{Tr} \text{Ln}\mathcal{G}^{-1} + T\text{Tr} \text{Ln}G_0^{-1} \right) \Big|_{\rho=const}. \quad (7)$$

The kinetic Ω_{kin} and potential Ω_{pot} parts are expressed through the Green function of the neutral fermions which obeys the equation

$$\left[-\hat{I}\partial_\tau + \tau_3 \left(\frac{\nabla^2}{2m} + \mu \right) + \tau_1 \rho \right] \mathcal{G}(\tau, \mathbf{r}) = \delta(\tau)\delta(\mathbf{r}) \quad (8)$$

and the operator

$$\Sigma(\partial\theta) \equiv \tau_3 \left[i\partial_\tau\theta + \frac{(\nabla\theta)^2}{2m} \right] - \hat{I} \left[\frac{i\nabla^2\theta}{2m} + \frac{i\nabla\theta(\tau, \mathbf{r})\nabla}{m} \right]. \quad (9)$$

The representation (5) allows one to get a full set of the equations which are necessary to find T_{BKT} , $\rho(T_{BKT})$ and $\mu(T_{BKT})$ at given ϵ_F (or, for example, $\rho(T)$ and $\mu(T)$ at given T and ϵ_F). While the equation for T_{BKT} will be written using the kinetic part (6) of the effective action, the equations for $\rho(T_{BKT})$ and $\mu(T_{BKT})$ (or $\rho(T)$ and $\mu(T)$) could be obtained using the mean field potential (7). It turns out that in the phase where $\rho \neq 0$ the mean-field approximation for the modulus variable describes the system quite well. This is mainly related with a nonperturbative character of the Hubbard-Stratonovich method, i.e. most of effects are taken over by a nonzero value of ρ .

III. DERIVATION OF THE EQUATION FOR T_{BKT}

If the model under consideration was reduced to a some known model describing the BKT phase transition, we would be easily write the equation for T_{BKT} . Indeed, in the lowest orders the kinetic term (6) coincides with classical spin XY-model [22,23] which has the following continuum Hamiltonian

$$H = \frac{J}{2} \int d\mathbf{r} [\nabla\theta(\mathbf{r})]^2. \quad (10)$$

Here J is the some constant (in the original classical discrete XY-model it is the stiffness of the relatively small spin rotations) and θ is the angle (phase) of the two-component vector in plane.

The temperature of the BKT transition is, in fact, known for this model, namely

$$T_{BKT} = \frac{\pi}{2}J. \quad (11)$$

Despite the very simple form ¹ of the equation (11), it was derived (see e.g. [22,23]) using the renormalization group technique, which takes into account the non-single-valuedness of the phase θ . Thus, the fluctuations of the phase are taken into account at a higher approximation than the Gaussian one ².

To expand Ω_{kin} up to $\sim (\nabla\theta)^2$, it would be sufficient to restrict ourselves to terms with $n = 1, 2$ in the expansion (6). The procedure of calculation (see Appendix B) is similar to that employed in [25], where the case of large densities n_f at $T = 0$ was considered, and gives ³

$$\Omega_{kin} = \frac{T}{2} \int_0^\beta d\tau \int d\mathbf{r} \left[J(\mu, T, \rho(\mu, T)) (\nabla\theta)^2 + K(\mu, T, \rho(\mu, T)) (\partial_\tau\theta)^2 \right], \quad (12)$$

where

$$J(\mu, T, \rho) = \frac{1}{m} n_F(\mu, T, \rho) - \frac{T}{\pi} \int_{-\mu/2T}^\infty dx \frac{x + \mu/2T}{\cosh^2 \sqrt{x^2 + \frac{\rho^2}{4T^2}}} \quad (13)$$

characterizes here the stiffness of the neutral order parameter,

$$K(\mu, T, \rho) = \frac{m}{2\pi} \left(1 + \frac{\mu}{\sqrt{\mu^2 + \rho^2}} \tanh \frac{\sqrt{\mu^2 + \rho^2}}{2T} \right), \quad (14)$$

and the value

$$n_F(\mu, T, \rho) = \frac{m}{2\pi} \left\{ \sqrt{\mu^2 + \rho^2} + \mu + 2T \ln \left[1 + \exp \left(-\frac{\sqrt{\mu^2 + \rho^2}}{T} \right) \right] \right\} \quad (15)$$

has a sense of fermi-quasiparticles density (for $\rho = 0$ the expression (15) is simply the density of the free fermions). Note that $J(\mu, T, \rho = 0) = 0$, or in other words the BKT boson disappears above T_ρ .

A direct comparison of the expression (12) with the Hamiltonian of XY-model (10) makes it possible to write directly the equation (11) for T_{BKT} :

¹The exponentially small correction is omitted here.

²Note that XY-model was recently supposed to be adequate for the qualitative description of the underdoped cuprates [24].

³A total derivative with respect to τ is omitted.

$$\frac{\pi}{2}J(\mu, T_{BKT}, \rho(\mu, T_{BKT})) = T_{BKT}. \quad (16)$$

Although mathematically the problem reduces to a well-known one, the analogy is incomplete. Indeed, in the standard XY-model (as well as the nonlinear σ -model) the vector (spin) subject to ordering is assumed to be a unit vector with no dependence⁴ on T . In our case this is fundamentally not the case, and a self-consistent calculation of T_{BKT} as a function of n_f requires additional equations for ρ and μ , which together with (16) form a complete system.

IV. SELF-CONSISTENT EQUATIONS FOR NEUTRAL ORDER PARAMETER AND CHEMICAL POTENTIAL

Using the definition (7), one can derive (see Appendix A) that

$$\Omega_{pot}(v, \mu, T, \rho) = v \left\{ \frac{\rho^2}{V} - \int \frac{d\mathbf{k}}{(2\pi)^2} \left[2T \ln \cosh \frac{\sqrt{\xi^2(\mathbf{k}) + \rho^2}}{2T} - \xi(\mathbf{k}) \right] \right\}, \quad (17)$$

where $\xi(\mathbf{k}) = \varepsilon(\mathbf{k}) - \mu$ with $\varepsilon(\mathbf{k}) = \mathbf{k}^2/2m$. Then the desired missing equations are the condition $\partial\Omega_{pot}(\rho)/\partial\rho = 0$ that the potential (17) be minimum and the equality $v^{-1}\partial\Omega_{pot}/\partial\mu = -n_f$, which fixes n_f . For them we have, respectively:

$$\frac{1}{V} = \int \frac{d\mathbf{k}}{(2\pi)^2} \frac{1}{2\sqrt{\xi^2(\mathbf{k}) + \rho^2}} \tanh \frac{\sqrt{\xi^2(\mathbf{k}) + \rho^2}}{2T}, \quad (18)$$

$$n_F(\mu, T, \rho) = n_f. \quad (19)$$

The equations (18) and (19) obtained above comprise a self-consistent system for determining the modulus ρ of the order parameter and the chemical potential μ in the mean-field approximation for fixed T and n_f .

The energy of two-particle bound states in a vacuum

$$\varepsilon_b = -2W \exp\left(-\frac{4\pi}{mV}\right) \quad (20)$$

(see [26,3,5]) is more convenient to use than the four-fermion constant V (here W is the conduction bandwidth). For example, one may easily go to the limits $W \rightarrow \infty$ and $V \rightarrow 0$ in the equation (18), which after this renormalization becomes

⁴There is no doubts that in certain situations (for example, very high T) it also can become a thermodynamical variable, i.e. dependent on T , as happens in problems of phase transitions between ordered (magnetic) and disordered (paramagnetic) phases when the spin itself vanishes. Specifically, for quasi-2D spin systems it is virtually obvious that as one proceeds from high- T regions, at first a spin modulus forms in 2D clusters of finite size and only then does global 3D ordering occur.

$$\ln \frac{|\varepsilon_b|}{\sqrt{\mu^2 + \rho^2} - \mu} = 2 \int_{-\mu/T}^{\infty} du \frac{1}{\sqrt{u^2 + \left(\frac{\rho}{T}\right)^2} \left[\exp \sqrt{u^2 + \left(\frac{\rho}{T}\right)^2} + 1 \right]}. \quad (21)$$

Thus, in practice, we will solve numerically the system of the equations (16), (21) and (19) to study T_{BKT} as function of n_f (or what is the same of ϵ_F).

It is easy to show that at $T = 0$ the system (21), (19) transforms into the system which was already addressed (see [3] and references therein). Recall that its solution is $\rho = \sqrt{2|\varepsilon_b|\epsilon_F}$ and $\mu = -|\varepsilon_b|/2 + \epsilon_F$. This will be useful for studying the concentration dependencies of $2\Delta/T_{BKT}$ and $2\Delta/T_\rho$, where Δ is the zero-temperature gap in the quasiparticle excitation spectrum. It should be kept in mind that in the local pair regime ($\mu < 0$) the gap Δ equals not ρ (as in the case $\mu > 0$) but rather $\sqrt{\mu^2 + \rho^2}$ [3].

Setting $\rho = 0$ in the equations (18) and (19), we arrive (in the same approximation) at the equations for the critical temperature T_ρ and the corresponding value of μ :

$$\ln \frac{|\varepsilon_b| \gamma}{T_\rho \pi} = - \int_0^{\mu/2T_\rho} du \frac{\tanh u}{u} \quad (\gamma = 1.781), \quad (22)$$

$$T_\rho \ln \left[1 + \exp \left(\frac{\mu}{T_\rho} \right) \right] = \epsilon_F, \quad (23)$$

where the Fermi energy $\epsilon_F = \pi n_f/m$ as it should be for 2D metals with the simplest quadratic dispersion law. Note that these equations coincide with the system which determines the mean-field temperature $T_c^{(2D)MF} (= T_\rho)$ and $\mu(T_c^{(2D)MF})$ (see [5]). This is evidently related with mean-field approximation used here. There is, however, a crucial difference between the temperatures T_c^{2D} and T_ρ . Namely, if one takes into account the fluctuations, the value of T_c^{2D} goes to zero, while the value of T_ρ remains finite. That is the reason why the temperature T_ρ has its own physical meaning: the incoherent (local or Cooper) pairs begin to be formed (at least at rather high n_f (see below Sec. VI)) just below T_ρ . At higher temperatures there are these pair fluctuations only (see e.g. [27]).

V. NUMERICAL RESULTS

The numerical investigation of the systems (16), (21), (19) and (22), (23) gives the following results, which are displayed graphically as the phase diagram of the system.

a) The pseudogap phase region (see Fig.1) in the present model is commensurate with the BKT region. But it has not been ruled out that in the case of the quasi-2D model this region will disappear as n_f increases due to formation of the phase with long-range order. For example, in the case of an indirect interaction it was shown [28] that the pseudogap phase region really exists at the relatively low carrier density only, i.e. it shrinks when the doping increases.

b) For low $\epsilon_F (\ll |\varepsilon_b|)$ the function $T_{BKT}(\epsilon_F)$ is linear, as it also confirmed by the analytical solution of the system (16), (21) and (19), which gives $T_{BKT} = \epsilon_F/2$. Surprisingly but namely such a behavior of T_c versus ϵ_F is observed for all families of HTSC cuprates in their underdoped region [2,24].

We note that in this limit the temperature T_c of formation of a homogeneous order parameter for the quasi-2D model [2,4] can be easily written in the following form

$$T_c \approx \frac{T_{BKT}}{\ln(\epsilon_F |\epsilon_b| / 4t_{||}^2)}, \quad (24)$$

where $t_{||}$ is the inter-plane hopping (coherent tunnelling) constant. This shows that when $T_c < T_{BKT}$ the weak three-dimensionalization can preserve (in any case, for low n_f) the regions of the pseudogap and BKT phases, which, for example, happens in the relativistic quasi-2D model [29]. At the same time, as the three-dimensionalization parameter $t_{||}$ increases, when $T_c > T_{BKT}$ the BKT phase can vanish, provide, however, that the anomalous phase region and both temperatures T_ρ and $T_c \simeq n_f/m$ are preserved. It follows from (24) that the BKT phase vanishes rather quickly when $t_{||} > \sqrt{2|\epsilon_b|\epsilon_F} (= \Delta)$.

c) Figure 2 shows the values n_f for which μ differs substantially from ϵ_F and, in other words, the Landau Fermi-liquid theory becomes inapplicable for metals (called also bad ones) with low or intermediate carrier density. As expected, the kink μ at $T = T_\rho$, experiments on observation which were discussed in [30] and have been interpreted for the 1-2-3 cuprate [31], becomes increasingly less pronounced as ϵ_F increases. But in the present case it is interesting that in the hydrodynamical approximation employed it happens at the normal-pseudogap phases boundary or before superconductivity really appears. Therefore it would be of great interest to perform experiments which would reveal the temperature dependence $\mu(T)$ especially for strongly anisotropic and relatively weakly doped cuprates.

d) It follows from curve 3 in Fig. 2 that the crossover (change in sign of μ) from local to Cooper pairs is possible not only as ϵ_F increases, which is more or less obvious, but also (for some n_f) as T increases.

e) Finally the calculations showed (see Fig. 3) that the ratio $2\Delta/T_{BKT}$ is always greater than 4.4. The value $2\Delta/T_\rho (= 2\Delta/T_c^{MF})$ is, however, somewhat lower and reaches the BCS theory limit of 3.52 only for $\epsilon_F \gg |\epsilon_b|$. It is interesting that this concentration behavior is consistent with numerous measurements of this ratio in HTSC [32,33]. Note that the divergencies of $2\Delta/T_{BKT}$ and $2\Delta/T_\rho$ at $\epsilon_F \rightarrow 0$ are directly related with the definition of Δ at $\mu < 0$.

VI. PAIRING TEMPERATURE T_P VERSUS CARRIER DENSITY

There are no disagreements if one concerns the asymptotic of T_{BKT} (or T_c) $\sim \epsilon_F$ in the region of the very low carrier densities. By contrast, the behavior of the temperature T_ρ , below which the pairs are formed, cannot be considered as generally accepted. For example, in the papers [2,24], proceeding from the qualitative arguments, this temperature is considered as the temperature T_P of local uncorrelated pairing, which in contrast to T_ρ increases with decreasing n_f ⁵. Randeria (see [3] and the references therein) to define the pairing temperature T_P uses the system of equations for the mean-field transition temperature and

⁵In fact, in the papers reminded (see also [34]) this temperature was plotted as an increasing function of coupling constant V that for 3D systems corresponds, to some extent, to the carrier

the corresponding chemical potential, which practically coincides with the system (22), (23). Thus his $T_P \rightarrow 0$ as $n_f \rightarrow 0$.

In our opinion the temperature T_ρ has its own physical sense, namely this is temperature of the phase transition to the state where the neutral order parameter $\rho \neq 0$ and below which one can observe the pseudogap manifestations. As to the temperature T_P , to define it properly one should study the spectrum of bound states solving the Bethe-Salpether equation [5] or analyzing the corresponding Green functions that we would like to do here. It turns out that, there is no difference between T_P and T_ρ in the Cooper pair regime ($\mu > 0$), while in the local pair region ($\mu < 0$) these temperatures have the different behavior.

Indeed, let us study the spectrum of bound states in both the normal ($\rho = 0$) and pseudogap ($\rho \neq 0$) phases. Especially we are interested in the determining conditions under which the real bound states (with zero total momentum $\mathbf{K} = 0$) become unstable. For this purpose one can look at the propagator of ρ -particle which is present in the pseudogap phase and is given by the following formula

$$\Gamma^{-1}(\tau, \mathbf{r}) = \frac{1}{2} \frac{\beta \delta^2 \Omega(v, \mu, T, \rho(\tau, \mathbf{r}), \partial \theta(\tau, \mathbf{r}))}{\delta \rho(\tau, \mathbf{r}) \delta \rho(0, 0)} \Big|_{\rho=\rho_{min}=const}, \quad (25)$$

where ρ_{min} is defined by the minimum condition (18) (or (21)) of the potential part (17) of the effective action (3). In the momentum representation the spectrum of bound states is determined usually by the condition

$$\Gamma_R^{-1}(\omega, \mathbf{K}) = 0, \quad (26)$$

where $\Gamma_R(\omega, \mathbf{K})$ is the retarded Green function obtained directly from the temperature Green function $\Gamma_R(i\Omega_n, \mathbf{K})$ using the procedure of analytical continuation $i\Omega_n \rightarrow \omega + i0$ [35]. Recall that such an analytical continuation must be performed after evaluating the sum over Matsubara frequencies. In the case of the total momentum $\mathbf{K} = 0$ one arrives at the following equation for the energy spectrum

$$\Gamma_R^{-1}(\omega, 0) = \frac{1}{V} + \frac{1}{2} \int \frac{d\mathbf{k}}{(2\pi)^2} \frac{\xi^2(\mathbf{k})}{\sqrt{\xi^2(\mathbf{k}) + \rho^2}} \frac{\tanh \sqrt{\xi^2(\mathbf{k}) + \rho^2}/2T}{\omega^2 - 4[\xi^2(\mathbf{k}) + \rho^2]} = 0. \quad (27)$$

From the explicit expression (27) for $\Gamma_R(\omega, 0)$ it is evident that this function has the branch cut for the frequencies

$$|\omega| \geq 2 \min \sqrt{\xi^2(\mathbf{k}) + \rho^2} = \begin{cases} 2\rho, & \mu \geq 0 \\ 2\sqrt{\mu^2 + \rho^2}, & \mu < 0. \end{cases} \quad (28)$$

Thus, the bound states can exist below this cut.

The real bound states do become decaying into two-fermion ones when the energy of the former collides the branch point $2 \min \sqrt{\xi^2(\mathbf{k}) + \rho^2}$. Since Γ_R^{-1} is a monotonically decreasing

density decreasing. In 2D systems, however, where as it is well-known two-particle bound states are formed without any threshold and similar conclusion about behavior $T_P(n_f)$ is problematical and must be checked independently.

function of ω^2 it has the unique solution $|\varepsilon_b| = 2\rho(T)$ at which Eq. (27) coincides exactly with mean-field approximation. And it becomes clear that for $\mu < 0$ we have real bound states with the energy $\varepsilon_b(T)$ below two-particle scattering continuum at $\omega = 2\sqrt{\mu^2 + \rho^2}$, while at $\mu \geq 0$ there are no stable bound states. The line $\mu(T, \epsilon_F) = 0$ in the T - ϵ_F plane at $\rho \neq 0$ separates the negative μ region where the local pairs exist from that one (positive μ) where the Cooper pairs only take place. This line (see Fig. 4) begins at the point $T = (e^\gamma/\pi)|\varepsilon_b| \approx 0.6|\varepsilon_b|$, $\epsilon_F \approx 0.39|\varepsilon_b|$ and ends at the point $T = 0$, $\epsilon_F = |\varepsilon_b|/2$. (The last point directly follows from the solution for zero temperature $\mu = -|\varepsilon_b|/2 + \epsilon_F$ [3,5].)

To find a similar line in the normal phase let consider the corresponding equation for the bound states in it. The propagator of these states (in imaginary time formalism) is defined as follows

$$\Gamma^{-1}(\tau, \mathbf{r}) = \frac{\beta\delta^2\Omega(v, \mu, T, \Phi(\tau, \mathbf{r}), \Phi^*(\tau, \mathbf{r}))}{\delta\Phi^*(\tau, \mathbf{r})\delta\Phi(0, 0)} \Big|_{\Phi=\Phi^*=0}. \quad (29)$$

In symmetrical (normal) phase where $\rho = 0$ we use again (see Sec. II) the initial auxiliary fields Φ and Φ^* . Then in the momentum representation (after the summation over Matsubara frequencies) one can come to

$$\Gamma^{-1}(i\Omega_n, \mathbf{K}) = \frac{1}{V} - \frac{1}{2} \int \frac{d\mathbf{k}}{(2\pi)^2} \frac{\tanh \xi_+(\mathbf{k}, \mathbf{K})/2T + \tanh \xi_-(\mathbf{k}, \mathbf{K})/2T}{\xi_+(\mathbf{k}, \mathbf{K}) + \xi_-(\mathbf{k}, \mathbf{K}) - i\Omega_n};$$

$$\xi_{\pm}(\mathbf{k}, \mathbf{K}) \equiv \frac{1}{2m} \left(\mathbf{k} \pm \frac{\mathbf{K}}{2} \right)^2 - \mu, \quad (30)$$

where \mathbf{k} is the relative momenta of the pair. The spectrum of the bound states can be given again by the equation (26). Using the energy ε_b (see Eq. (20)) of the bound state at $T = 0$, and for $\mathbf{K} = 0$ from (30) we have the following equation for the energies of these states in the normal phase

$$\int_0^\infty \left[\frac{1}{x + |\varepsilon_b|/2} - \frac{\tanh(x - \mu)/2T}{x - \mu - \omega/2} \right] = 0. \quad (31)$$

It is seen that such states can exist provided $-2\mu - |\varepsilon_b| < \omega < -2\mu$. The left-hand side of Eq.(31) takes a positive value at $\omega = -2\mu - |\varepsilon_b|$ and tends to $+\infty$ ($\mu > 0$) or $-\infty$ ($\mu < 0$) when $\omega \rightarrow -2\mu$. This equation always has a solution at $\mu < 0$ what means that here bound states with zero total momentum exist for negative μ .

As to the region $\mu > 0$ the analysis here becomes a little bit complicated. It shows that bound states can exist here at least up to $\mu < |\varepsilon_b|/8$ [5]. But approximately the trajectory $\mu(T, \epsilon_F) = 0$ (or $T = \epsilon_F/\ln 2$, see (23)) also divides the normal phase on two qualitatively different regions – with ($\mu < 0$) and without ($\mu > 0$) stable (long-living) pairs. The same as was shown above takes place for another phases, what allows to draw the whole line $\mu(T, \epsilon_F) = 0$ (Fig. 4).

Knowing the binding two-particle energy it is naturally to define pairing temperature T_P as $T_P \approx |\varepsilon_b(T_P, \mu(T_P, \epsilon_F))|$. This equation can be easily analyzed in the region $\epsilon_F \ll |\varepsilon_b|$ for which we directly obtain $T_P \approx |\varepsilon_b|$ what evidently coincides with the standard estimation [2,36]. It means in its turn that the curve $T_P(\epsilon_F)$ starting at $T_P(0) \approx |\varepsilon_b|$ will be lowered up to the point $T_P(0.39\epsilon_F) \approx 0.6|\varepsilon_b|$ lying on the line $T_\rho(\epsilon_F)$ (see Fig. 4). It is important

that this line is not the phase transition one and divides the fermion system diagram on the temperature regions with prevailing mean number of local pairs ($T \lesssim T_P$) or unbounded carriers ($T \gtrsim T_P$). Just this region of *abnormal normal phase* should be expected to be responsible for anomalies observed in underdoped HTSC. This phase area or the difference $T_P(\epsilon_F) - T_\rho(\epsilon_F)$ is the growing function as $\epsilon \rightarrow 0$ what completely corresponds to the usually supposed its behavior [2,24].

When $\mu > 0$ there are no bound states $\varepsilon_b(T) = 2\rho(T) = 0$ for the normal phase where they are short-living. Formally, using $\rho(T) = 0$ in the Eq. (27) we immediately come to (22) or, in other words, here $T_P = T_\rho$. Such a conclusion is in a complete accordance with generally accepted definition of T_P in the BCS case [36].

Thus the phase diagram of 2D metal above T_c acquires the form shown in Fig. 4. It is interesting that if the line $T_P(\epsilon_F)$ cannot be defined exactly, the temperature $T_\rho(\epsilon_F)$ is the line of the phase transition when the pairs reveal some signs of collective behavior. Moreover, namely at $T < T_\rho$ one can say about real pseudogap in the one-particle spectrum, while in the region $T_\rho < T < T_P$ only strongly developed pair fluctuations (some number of pairs) exist, though they can be probably sufficient for lowering of spectral quasi-particle weight and other observed manifestation masking pseudogap (spin gap, see [27]) formation.

VII. PARAMAGNETIC SUSCEPTIBILITY OF THE SYSTEM

It would be very interesting to study how a nonzero value of the neutral order parameter affects the observable properties of the 2D system. Does this really resemble the gap opening in the traditional superconductors, except that it happens in the normal phase? Or, in other words, does the pseudogap open?

We shall demonstrate this phenomenon taking, as the simplest case in point, the paramagnetic susceptibility of the system. To study the system in the magnetic field \mathbf{H} one has to add the paramagnetic term

$$\mathcal{H}_{PM} = -\mu_B H \left[\psi_\uparrow^\dagger(\mathbf{r})\psi_\uparrow(\mathbf{r}) - \psi_\downarrow^\dagger(\mathbf{r})\psi_\downarrow(\mathbf{r}) \right], \quad (32)$$

where $\mu_B = e\hbar/2mc$ is the Bohr magneton, to the Hamiltonian (1). Note that, using the isotropy in the problem, we chose the direction of field \mathbf{H} to be perpendicular to the plane containing the vectors \mathbf{r} .

Adding the corresponding term to the equation (8) for the neutral fermion Green function, it is easy to obtain that of in the momentum representation (compare with(B.2))

$$\mathcal{G}(i\omega_n, \mathbf{k}, \vec{H}) = \frac{(i\omega_n + \mu_B H)\hat{I} + \tau_3 \xi(\mathbf{k}) - \tau_1 \rho}{(i\omega_n + \mu_B H)^2 - \xi^2(\mathbf{k}) - \rho^2}. \quad (33)$$

The static paramagnetic susceptibility is expressed through the magnetization

$$\chi(\mu, T, \rho) = \left. \frac{\partial M(\mu, T, \rho, \vec{H})}{\partial H} \right|_{H=0}, \quad (34)$$

which in the mean-field approximation may be derived from the effective potential

$$M(\mu, T, \rho, \vec{H}) = -\frac{1}{v} \frac{\partial \Omega_{pot}(v, \mu, T, \rho, \vec{H})}{\partial H}. \quad (35)$$

Thus from (35) one obtains

$$M(\mu, T, \rho, \vec{H}) = \mu_B T \sum_{n=-\infty}^{\infty} \int \frac{d\mathbf{k}}{(2\pi)^2} \text{tr}[\mathcal{G}(i\omega_n, \mathbf{k}, \vec{H}) \hat{I}]. \quad (36)$$

Then using the definition (34) one arrives at

$$\chi(\mu, T, \rho) = \mu_B^2 \int \frac{d\mathbf{k}}{(2\pi)^2} 2T \sum_{n=-\infty}^{\infty} \frac{\xi^2(\mathbf{k}) + \rho^2 - \omega_n^2}{[\omega_n^2 + \xi^2(\mathbf{k}) + \rho^2]^2}. \quad (37)$$

The sum in (37) is calculated in Appendix C (see the equation (C.5)) and, thus, we obtain the final result

$$\chi(\mu, T, \rho) = \chi_{Pauli} \frac{1}{2} \int_{-\mu/2T}^{\infty} \frac{dx}{\cosh^2 \sqrt{x^2 + \frac{\rho^2}{4T^2}}}, \quad (38)$$

where $\chi_{Pauli} \equiv \mu_B^2 m / \pi$ is the Pauli paramagnetic susceptibility for the 2D system.

To study χ as a function of T and n_f (or ϵ_F) the formula (38) should be used together with the equations (21) and (19).

For the case of the normal phase ($\rho = 0$) one can investigate the system analytically. Thus (38) takes form

$$\chi(\mu, T, \rho = 0) = \chi_{Pauli} \frac{1}{1 + \exp(-\mu/T)}, \quad (39)$$

while μ is already determined by (23). This system has the solution

$$\chi(\epsilon_F, T, \rho = 0) = \chi_{Pauli} [1 - \exp(-\epsilon_F/T)], \quad (40)$$

which identically coincides with that known from the literature [37].

The results of numerical study of the system (38), (21) and (19) are presented in Fig. 5. One can see that the kink in χ happens at $T = T_\rho$ as in the dependence of μ on T . Below T_ρ the value of $\chi(T)$ decreases, although the system is still normal. This can be interpreted as the spin-gap (or pseudogap) opening. The size of the pseudogap region depends strongly on the doping ($\epsilon_F/|\epsilon_b|$), as it takes place for the real HTSC [17,18,16]. For small values of $\epsilon_F/|\epsilon_b|$ this region is large ($T_\rho > 2T_{BKT}$), while for the large ratio it is small.

VIII. CONCLUSION

To summarize we have discussed the crossover in the superconducting transition between BCS- and Bose-like behavior for simplest 2D model with s-wave nonretarded attractive interaction.

While there is still no generally accepted microscopic theory of HTSC compounds and their basic features (including the pairing mechanism), it seems that this approach, although

in a sense phenomenological, is of great interest since it is able to cover the whole region of carrier concentrations (and consequently the whole range of coupling constants), temperatures. It, as we tried to demonstrate, allows one not only to propose a reasonable interpretation for the observed phenomena caused by doping but also to predict new phenomena (for example, pseudogap phase formation as a new thermodynamically equilibrium normal state of low dimensional conducting electronic systems).

Evidently there are a number of important open questions. They may be divided into two classes: the first one concerns the problem of a better and more complete treatment of the models themselves. The second class is related to the problem of to what extent this model is applicable to HTSC compounds and what are the necessary ingredients for a more realistic description.

Regarding the microscopic Hamiltonian as a given model, it is obvious that our treatment is still incomplete. In particular there is some unconfirmed numerical result [38] based on a fully self-consistent determination of a phase transition to a superconducting state in a conserving approximation, which states that the superconducting transition is neither the simple mean-field transition nor the BKT transition. Besides, it would be very interesting to obtain the spectrum of the both anomalous normal and pseudogap phases.

Concerning the question to which the models considered are really applicable to HTSC, it is obvious that most of the complexity of these systems is neglected here. We did not take into account a possible indirect nature of the interaction between the fermions, now widely discussed (see [39,14,40]) d-wave pairing, inter-layer tunnelling, etc.

ACKNOWLEDGMENTS

We would like to thank Drs. E.V. Gorbar, I.A. Shovkovy and V.M. Turkowski for the fruitful discussions which helped to make clear some deep questions of the low dimensional phase transitions. Particularly we thank Prof. R.M. Carter for many thoughtful comments on the earlier version of this manuscript. One of us (S.G.Sh) is grateful to the members of the Department of Physics of the University of Pretoria, especially Prof. R.M. Carter and Dr. N.J. Davidson, for very useful points and hospitality.

APPENDIX A: KINETIC PART OF THE EFFECTIVE ACTION IN THE LOW ENERGY LIMIT

Here we derive the kinetic part (6) of the effective action (5). To obtain it one should calculate directly the first two terms of the series in (6) which are formally written as $\Omega_{kin}^{(1)} = T\text{Tr}(\mathcal{G}\Sigma)$ and $\Omega_{kin}^{(2)} = \frac{1}{2}T\text{Tr}(\mathcal{G}\Sigma\mathcal{G}\Sigma)$. The straightforward calculation of $\Omega_{kin}^{(1)}$ gives

$$\Omega_{kin}^{(1)} = T \int_0^\beta d\tau \int d\mathbf{r} \frac{T}{(2\pi)^2} \sum_{n=-\infty}^{\infty} \int d\mathbf{k} \text{tr}[\mathcal{G}(i\omega_n, \mathbf{k})\tau_3] \left(i\partial_\tau\theta + \frac{(\nabla\theta)^2}{2m} \right), \quad (\text{A.1})$$

where

$$\mathcal{G}(i\omega_n, \mathbf{k}) = -\frac{i\omega_n\hat{I} + \tau_3\xi(\mathbf{k}) - \tau_1\rho}{\omega_n^2 + \xi^2(\mathbf{k}) + \rho^2} \quad (\text{A.2})$$

is the Green function of the neutral fermions in the frequency-momentum representation. The summation over Matsubara frequencies $\omega_n = \pi(2n+1)T$ and integration over \mathbf{k} in (A.1) can be easily performed using the sum (B.8) and thus one obtains

$$\Omega_{kin}^{(1)} = T \int_0^\beta d\tau \int d\mathbf{r} n_F(\mu, T, \rho) \left(i\partial_\tau \theta + \frac{(\nabla\theta)^2}{2m} \right), \quad (\text{A.3})$$

where $n_F(\mu, T, \rho)$ is determined by (15). We note that Σ has the following structure $\Sigma = \tau_3 O_1 + \hat{I} O_2$ where O_1 and O_2 are some differential operators (see (9)). One can see, however, that the part of Σ , proportional to the unit matrix \hat{I} , does not contribute in $\Omega_{kin}^{(1)}$.

For the case $T = 0$ [21,25] when real time t replaces imaginary time τ , one can argue from the Galilean invariance that the coefficient of $\partial_t \theta$ is rigidly related to the coefficient at $(\nabla\theta)^2$. So it does not appear in $\Omega_{kin}^{(2)}$. We wish, however, to stress that these arguments can not be used to exclude the appearance of the term $(\nabla\theta)^2$ from $\Omega_{kin}^{(2)}$ when $T \neq 0$, thus we must calculate it explicitly.

The O_1 term in Σ yields

$$\Omega_{kin}^{(2)}(O_1) = \frac{T}{2} \int_0^\beta d\tau \int d\mathbf{r} \frac{T}{(2\pi)^2} \sum_{n=-\infty}^{\infty} \int d\mathbf{k} \text{tr}[\mathcal{G}(i\omega_n, \mathbf{k}) \tau_3 \mathcal{G}(i\omega_n, \mathbf{k}) \tau_3] \left(i\partial_\tau \theta + \frac{(\nabla\theta)^2}{2m} \right)^2, \quad (\text{A.4})$$

And from (A.4) we find that

$$\Omega_{kin}^{(2)}(O_1) = -\frac{T}{2} \int_0^\beta d\tau \int d\mathbf{r} K(\mu, T, \rho) \left(i\partial_\tau \theta + \frac{(\nabla\theta)^2}{2m} \right)^2, \quad (\text{A.5})$$

where $K(\mu, T, \rho)$ was defined in (14). It is evident that O_1 term does not affect the coefficient of $(\nabla\theta)^2$. Further, it is easy to make sure that the cross term from O_1 and O_2 in $\Omega_{kin}^{(2)}$ is absent. Finally, the calculations of the O_2 term contribution to $\Omega_{kin}^{(2)}$ ⁶ give

$$\Omega_{kin}^{(2)}(O_2) = T \int_0^\beta d\tau \int d\mathbf{r} \frac{T}{(2\pi)^2} \sum_{n=-\infty}^{\infty} \int d\mathbf{k} \mathbf{k}^2 \text{tr}[\mathcal{G}(i\omega_n, \mathbf{k}) \hat{I} \mathcal{G}(i\omega_n, \mathbf{k}) \hat{I}] \frac{(\nabla\theta)^2}{4m^2}. \quad (\text{A.6})$$

Thus, after summation over Matsubara frequencies (see Appendix C)

$$\Omega_{kin}^{(2)}(O_2) = - \int_0^\beta d\tau \int d\mathbf{r} \frac{1}{32\pi^2 m^2} \int d\mathbf{k} \frac{\mathbf{k}^2}{\cosh^2 \frac{\sqrt{\xi^2(\mathbf{k}) + \rho^2}}{2T}} (\nabla\theta)^2. \quad (\text{A.7})$$

As expected this term vanishes when $T \rightarrow 0$ but at finite T it is comparable with (A.3). Combining (A.3), (A.5) and (A.7) we obtain (12).

⁶The higher than $(\nabla\theta)^2$ derivatives were not found here.

APPENDIX B: THE CALCULATION OF THE EFFECTIVE POTENTIAL

Let us derive the effective potential (17). To obtain it one should write down the formal expression (7) in the momentum representation, so that

$$\begin{aligned} \Omega_{pot}(v, \mu, T, \rho) = v \left\{ \frac{\rho^2}{V} - T \sum_{n=-\infty}^{+\infty} \int \frac{d\mathbf{k}}{(2\pi)^2} \text{tr}[\ln G^{-1}(i\omega_n, \mathbf{k}) e^{i\delta\omega_n\tau_3}] \right. \\ \left. + T \sum_{n=-\infty}^{+\infty} \int \frac{d\mathbf{k}}{(2\pi)^2} \text{tr}[\ln G_0^{-1}(i\omega_n, \mathbf{k}) e^{i\delta\omega_n\tau_3}] \right\}, \quad \delta \rightarrow +0, \end{aligned} \quad (\text{B.1})$$

where

$$G^{-1}(i\omega_n, \mathbf{k}) = i\omega_n \hat{I} - \tau_3 \xi(\mathbf{k}) + \tau_1 \rho \quad (\text{B.2})$$

and

$$G_0^{-1}(i\omega_n, \mathbf{k}) = G^{-1}(i\omega_n, \mathbf{k}) \Big|_{\rho=\mu=0} \quad (\text{B.3})$$

are the inverse Green functions. The exponential factor $e^{i\delta\omega_n\tau_3}$ is added into (B.1) to provide a right regularization which is necessary to perform the calculation with the Green functions (see [35]). For instance, one obtains that

$$\begin{aligned} \lim_{\delta \rightarrow +0} \sum_{n=-\infty}^{+\infty} \text{tr}[\ln G^{-1}(i\omega_n, \mathbf{k}) e^{i\delta\omega_n\tau_3}] = \\ \lim_{\delta \rightarrow +0} \left\{ \sum_{n=-\infty}^{+\infty} \text{tr}[\ln G^{-1}(i\omega_n, \mathbf{k})] \cos \delta\omega_n + \right. \\ \left. i \sum_{\omega_n > 0} \sin \delta\omega_n \text{tr}[(\ln G^{-1}(i\omega_n, \mathbf{k}) - \ln G^{-1}(-i\omega_n, \mathbf{k}))\tau_3] \right\} = \\ \sum_{n=-\infty}^{+\infty} \text{tr}[\ln G^{-1}(i\omega_n, \mathbf{k})] - \frac{\xi(\mathbf{k})}{T}, \end{aligned} \quad (\text{B.4})$$

where the properties that

$$\ln G^{-1}(i\omega_n, \mathbf{k}) = -\tau_3 \frac{\xi(\mathbf{k})}{i\omega_n}, \quad \omega_n \rightarrow \infty$$

and

$$\sum_{\omega_n > 0} \frac{\sin \delta\omega_n}{\omega_n} \simeq \frac{1}{2\pi T} \int_0^\infty dx \frac{\sin \delta x}{x} = \frac{1}{4T} \text{sign} \delta$$

were used.

To calculate the sum in (B.4) one has firstly to use the identity $\text{tr} \ln \hat{A} = \ln \det \hat{A}$, so that (B.1) takes the following form

$$\Omega_{pot}(v, \mu, T, \rho) = v \left\{ \frac{\rho^2}{V} - T \sum_{n=-\infty}^{+\infty} \int \frac{d\mathbf{k}}{(2\pi)^2} \ln \frac{\det G^{-1}(i\omega_n, \mathbf{k})}{\det G_0^{-1}(i\omega_n, \mathbf{k})} - \int \frac{d\mathbf{k}}{(2\pi)^2} [-\xi(\mathbf{k}) + \varepsilon(\mathbf{k})] \right\}. \quad (\text{B.5})$$

Calculating the determinants of the Green functions (B.2) and (B.3) one gets

$$\Omega_{pot}(v, \mu, T, \rho) = v \left\{ \frac{\rho^2}{V} - T \sum_{n=-\infty}^{+\infty} \int \frac{d\mathbf{k}}{(2\pi)^2} \ln \frac{\omega_n^2 + \xi^2(\mathbf{k}) + \rho^2}{\omega_n^2 + \varepsilon^2(\mathbf{k})} - \int \frac{d\mathbf{k}}{(2\pi)^2} [-\xi(\mathbf{k}) + \varepsilon(\mathbf{k})] \right\}, \quad (\text{B.6})$$

where the role of $G_0(i\omega_n, \mathbf{k})$ in the regularization of Ω_{pot} is evident now. The summation in (B.6) can be done if one uses the following representation

$$\ln \frac{\omega_n^2 + a^2}{\omega_n^2 + b^2} = \int_0^\infty dx \left(\frac{1}{\omega_n^2 + a^2 + x} - \frac{1}{\omega_n^2 + b^2 + x} \right). \quad (\text{B.7})$$

Then, the sum [41]

$$\sum_{k=0}^{\infty} \frac{1}{(2k+1)^2 + c^2} = \frac{\pi}{4c} \tanh \frac{\pi c}{2} \quad (\text{B.8})$$

may be now applied and one obtains

$$\ln \frac{\omega_n^2 + a^2}{\omega_n^2 + b^2} = \int_0^\infty dx \left(\frac{1}{2\sqrt{b^2 + x}} \tanh \frac{\sqrt{b^2 + x}}{2T} - \frac{1}{2\sqrt{a^2 + x}} \tanh \frac{\sqrt{a^2 + x}}{2T} \right). \quad (\text{B.9})$$

Integrating (B.9) over x one thus arrives to the expression:

$$T \sum_{n=-\infty}^{+\infty} \int \frac{d\mathbf{k}}{(2\pi)^2} \ln \frac{\omega_n^2 + \xi^2(\mathbf{k}) + \rho^2}{\omega_n^2 + \varepsilon^2(\mathbf{k})} = 2T \int \frac{d\mathbf{k}}{(2\pi)^2} \ln \frac{\cosh[\sqrt{\xi^2(\mathbf{k}) + \rho^2}/2T]}{\cosh[\varepsilon(\mathbf{k})/2T]}. \quad (\text{B.10})$$

Finally, substituting (B.10) into (B.6) we get (17), where the term which does not depend on ρ and μ is already omitted.

APPENDIX C: CALCULATION OF THE MATSUBARA FREQUENCY SUM

Here we perform the summation over Matsubara frequencies in the following expression

$$T \sum_{n=-\infty}^{\infty} \text{tr}[\mathcal{G}(i\omega_n, \mathbf{k}) \hat{I} \mathcal{G}(i\omega_n, \mathbf{k}) \hat{I}], \quad (\text{C.1})$$

where the Green function $\mathcal{G}(i\omega_n, \mathbf{k})$ is given by (A.2). At first, using the elementary properties of the Pauli matrices one obtains

$$\text{tr}[\mathcal{G}(i\omega_n, \mathbf{k}) \hat{I} \mathcal{G}(i\omega_n, \mathbf{k}) \hat{I}] = \frac{2[\xi^2(\mathbf{k}) + \rho^2 - \omega_n^2]}{[\omega_n^2 + \xi^2(\mathbf{k}) + \rho^2]^2}. \quad (\text{C.2})$$

Then, the summation can be easily carried out, if one uses the following sums [41]

$$\sum_{k=0}^{\infty} \frac{1}{[(2k+1)^2 + a^2]^2} = \frac{\pi}{8a^3} \tanh \frac{\pi a}{2} - \frac{\pi^2}{16a^2} \frac{1}{\cosh^2 \frac{\pi a}{2}} \quad (\text{C.3})$$

and

$$\sum_{k=0}^{\infty} \frac{(2k+1)^2}{[(2k+1)^2 + a^2]^2} = \frac{\pi}{8a} \tanh \frac{\pi a}{2} + \frac{\pi^2}{16} \frac{1}{\cosh^2 \frac{\pi a}{2}}. \quad (\text{C.4})$$

Assuming that $a^2 \equiv (\xi^2(\mathbf{k}) + \rho^2)/\pi^2 T^2$ one directly arrives to the final result

$$2T \sum_{n=-\infty}^{\infty} \frac{\xi^2(\mathbf{k}) + \rho^2 - \omega_n^2}{[\omega_n^2 + \xi^2(\mathbf{k}) + \rho^2]^2} = -\frac{1}{2T} \frac{1}{\cosh^2 \frac{\sqrt{\xi^2(\mathbf{k}) + \rho^2}}{2T}}. \quad (\text{C.5})$$

REFERENCES

- [1] V.M. Loktev, *Low Temp. Phys.* **22**, 1 (1996).
- [2] Y.J. Uemura, Preprint cond-mat/9706151, to be published in *Physica C*.
- [3] M. Randeria, in *Bose Einstein Condensation*, edited by A. Griffin, D.W. Snoke, and S. Stringari (Cambridge U.P. New Yourk, 1995) p.355.
- [4] E.V. Gorbar, V.M. Loktev, S.G. Sharapov, *Physica C* **257**, 355 (1996).
- [5] E.V. Gorbar, V.P. Gusynin, V.M. Loktev, *Low Temp. Phys.* **19**, 832 (1993);
Superconductivity: Physics, Chemistry, Technology **6**, 375 (1993);
 Preprint ITP-92-54E, Kiev, 1992.
- [6] N.D. Mermim, H. Wagner, *Phys. Rev. Lett.* **17**, 1113 (1966);
 P.C. Hohenberg, *Phys. Rev.* **158**, 383 (1967);
 S. Coleman, *Comm. Math. Phys.* **31**, 259 (1973).
- [7] S. Schmitt-Rink, C.M. Varma, A.E. Ruckenstein, *Phys. Rev. Lett.* **63**, 445 (1989).
- [8] J. Serene, *Phys. Rev. B* **40**, 10873 (1989).
- [9] A. Tokumitsu, K. Miyake, K. Yamada, *Phys. Rev. B* **47**, 11988 (1993).
- [10] P. Nozieres, S. Schmitt-Rink, *J. Low.Temp. Phys.* **59**, 195 (1985).
- [11] S.V. Traven, *Phys. Rev. Lett.* **73**, 3451 (1994).
- [12] R. MacKenzie, P.K. Panigrahi, S. Sakhi, *Int. J. Mod. Phys. A* **9**, 3603 (1994).
- [13] M. Drechsler, W. Zwerger, *Ann. Phys. (Germany)* **1**, 15 (1992).
- [14] S. Stintzing, W. Zwerger, Preprint cond-mat/9703129.
- [15] V.M. Loktev, Yu.G.Pogorelov, *Physica C* **272**, 151 (1996).
- [16] D. Pines, *Tr.J. of Physics* **20**, 535 (1996).
- [17] B.G. Levi, *Physics Today* **49**, 17 (1996).
- [18] H. Ding, T. Yokoya, I.C. Campuzano et al., *Nature* **382**, 51 (1996).
- [19] V.P. Gusynin, V.M. Loktev, S.G. Sharapov, *JETP Lett.* **65**, 182 (1997).
- [20] E. Witten, *Nucl. Phys. B* **145**, 110 (1978).
- [21] I.J.R. Aitchison, P. Ao, D.J. Thouless, X.-M. Zhu, *Phys. Rev. B* **51**, 6531 (1995).
- [22] Yu.A. Izyumov, Yu.N. Skryabin, *Statistical Mechanics of Magnetically Ordered Systems*, (Nauka, Moscow, 1987). Ch.15. (in Russian)
- [23] P. Minnhagen, *Rev. Mod. Phys.* **59**, 1001 (1987).
- [24] V. Emery, S.A. Kivelson, *Nature* **374**, 434 (1995); *Phys. Rev. Lett.* **74**, 3253 (1995).
- [25] A.M.J. Schakel, *Mod. Phys. Lett. B* **4**, 927 (1990).
- [26] K. Miyake, *Progr. Theor. Phys.* **69**, 1794 (1983).
- [27] V.M. Loktev, S.G. Sharapov, *Low Temp. Phys.* **23**, 132 (1997).
- [28] V.M. Loktev, S.G. Sharapov, V.M. Turkowski, Preprint cond-mat/9703070, to be published in *Physica C*.
- [29] H. Yamamoto, I. Ichinose, *Nucl. Phys.* **B370**, 695 (1992).
- [30] D. van der Marel, *Physica C* **165**, 35 (1990).
- [31] A.V. Dotsenko, O.P. Sushkov, Preprint cond-mat/9601031.
- [32] T.P. Devereaux, *Phys. Rev. Lett.* **74**, 4313 (1995).
- [33] C. Kendziora et al., *Phys. Rev. Lett.* **77**, 727 (1996).
- [34] R. Haussmann, *Phys. Rev. B* **49**, 12975 (1994).
- [35] A.A. Abrikosov, L.P. Gorkov, I.E. Dzyaloshinski, *Methods of Quantum Field Theory in Statistical Physics*, (Dover, 1975).

- [36] R. Micnas, T. Kostyrko, in *Proceedings of 1st Polish-US Conference*, Wroclaw, Poland, 11-15 September 1995.
- [37] I.A. Kvasnikov, *Thermodynamic and Statistical Physics*, (Moscow University Press, Moscow, 1991). (in Russian)
- [38] J.J. Deisz, D.W. Hess, J.W. Serene, Preprint cond-mat/9706012.
- [39] D.J. Scalapino, Phys. Rep. **250**, 329 (1995).
- [40] J.N. Engelbrecht, A. Nazarenko, M. Randeria, E. Dagotto, Preprint cond-mat/9705166.
- [41] A.P. Prudnikov, Yu.A. Brychkov, Yu.A. Marychev, *Integrals and Series. Elementary functions*, (Nauka, Moscow, 1981).

FIGURES

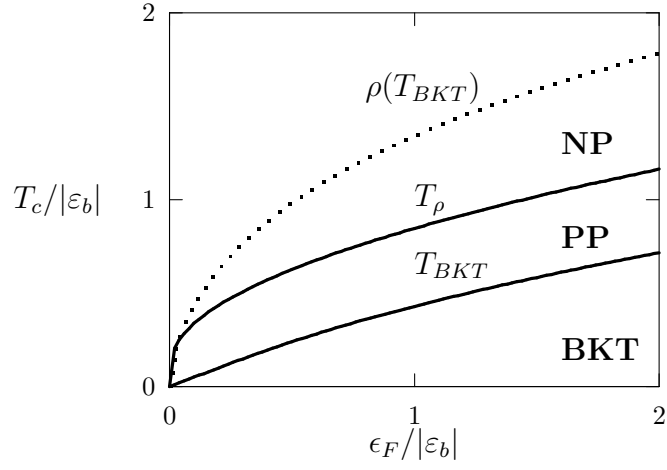


FIG. 1. T_{BKT} and T_ρ versus the noninteracting fermion density. The dots represent the function $\rho(\epsilon_F)$ at $T = T_{BKT}$. The regions of the normal phase (NP), pseudogap phase (PP) and BKT phase are indicated.

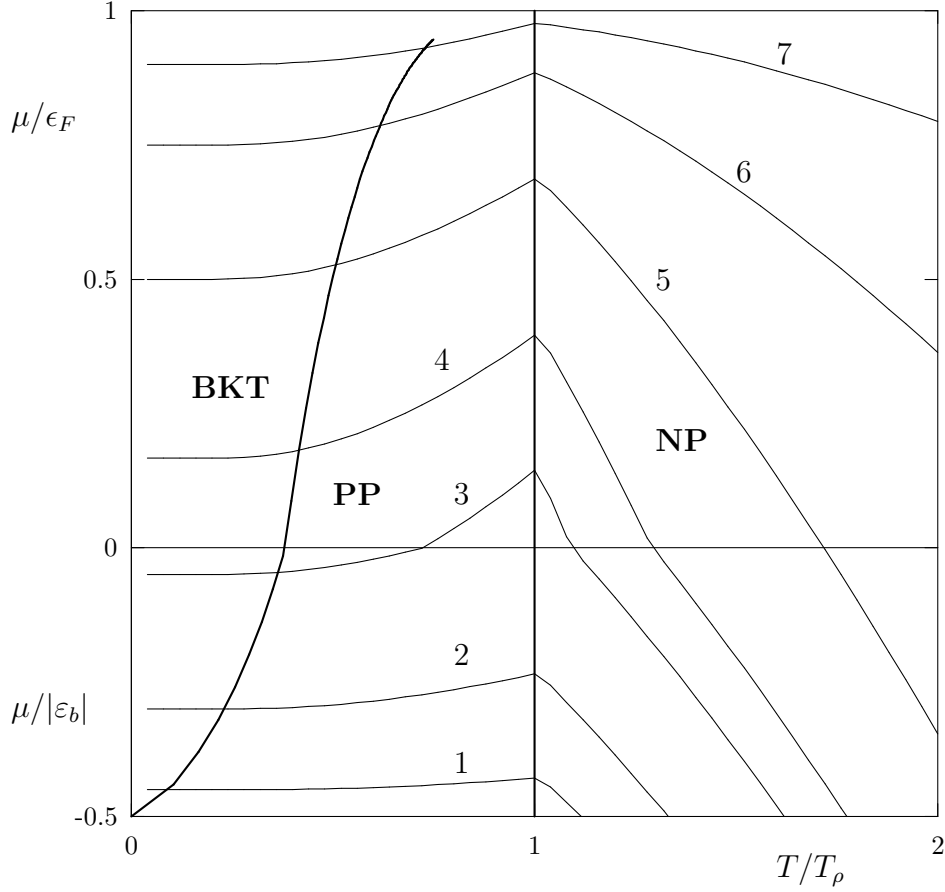


FIG. 2. $\mu(T)$ for different values of $\epsilon_F/|\epsilon_b|$: 1 — 0.05; 2 — 0.2; 3 — 0.45; 4 — 0.6; 5 — 1; 6 — 2; 7 — 5. (For $\mu > 0$ and $\mu < 0$ the chemical potential was scaled to ϵ_F and $|\epsilon_b|$, respectively.) The thick lines bound regions of the BKT, pseudogap (PP) and normal (NP) phases.

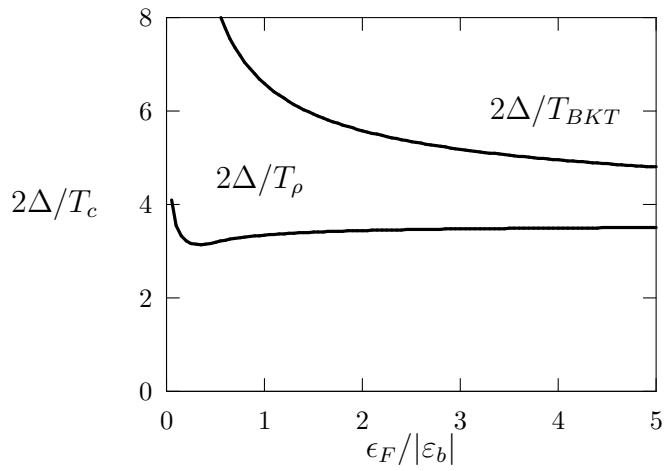


FIG. 3. $2\Delta/T_{BKT}$ and $2\Delta/T_\rho$ versus the non-interacting fermion density.

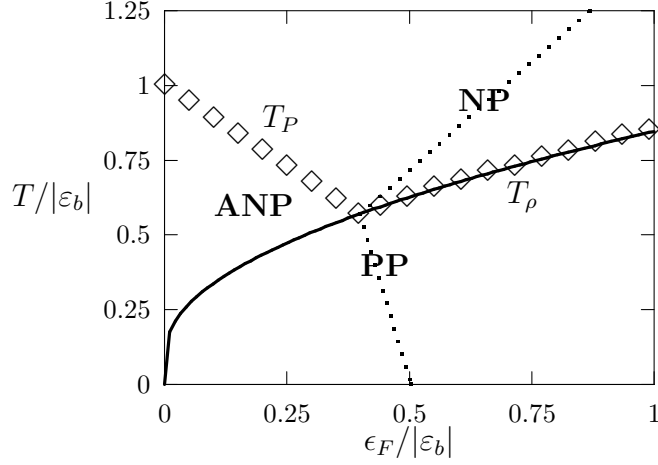


FIG. 4. Phase diagram of the 2D metal in the small concentration region. The dotted line corresponds to $\mu = 0$, and the temperature T_P separates abnormal normal phase (ANP) from normal one. The critical temperature T_{BKT} is not shown.

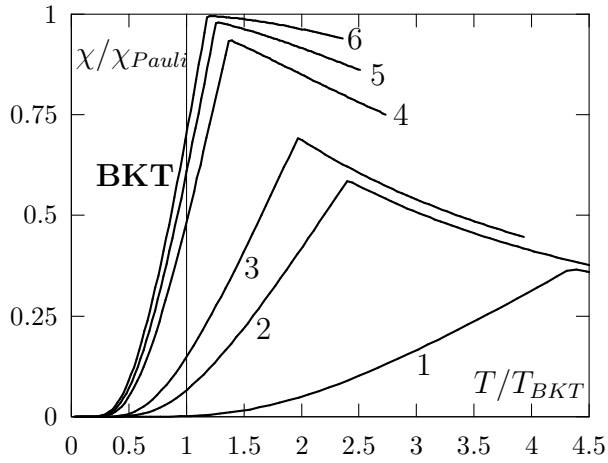


FIG. 5. $\chi(T)$ for different values of $\epsilon_F/|\epsilon_b|$: 1 — 0.2; 2 — 0.6; 3 — 1; 4 — 5; 5 — 10; 6 — 20.